Elementary Chemical Reactions of Acetylcholine with Receptor and Esterase: Relationship to Neuronal Information Transfer

EBERHARD NEUMANN
Max-Planck-Institut für Biochemie, D-8033 München, West Germany

TERRONE L. ROSENBERRY AND HAI WON CHANG
Departments of Neurology and Biochemistry College of Physicians and Surgeons Columbia University, New York, New York

I. INTRODUCTION

This chapter examines some conceptual problems involving neuronal information transfer mediated by acetylcholine. As is well known, acetylcholine is crucially involved in the control of ionic conductivities of nerve and muscle cell membranes. These membranes are intrinsically associated with two proteins which are essential for the cholinergic control of ion flows: (1) The acetylcholine receptor system "translates" the binding of acetylcholine into permeability changes (opening and closing of ion pathways, e.g., ion channels) in excitable membranes. (2) The enzyme acetylcholinesterase limits the duration of the acetylcholine action by hydrolytic removal of the activator from the membrane environment.

Mechanistic details of the coupling of acetylcholine reactions with these proteins to the membrane permeability changes are not known.

ISBN 0-12-398450-5

However, a useful hypothesis of the coupling mechanism was introduced by David Nachmansohn some 30 years ago (1). Central to this hypothesis was Nachmansohn's proposal in 1953 that the binding of acetylcholine induces a conformation change in the membrane-bound acetylcholine receptor (1–5). The conformation change was postulated to release receptor-bound Ca^{2+} ions which subsequently triggered a conductance increase through specific ion pathways in the membrane (4). The proposed conformation change may be represented by the reaction scheme in Fig. 1 The receptor form R corresponds to the closed or nonconducting state and the form R′, to the open or conducting state. In the absence of activator A, the closed conformation R is dominant; the ratio of the concentrations of receptor forms [R′]/[R] is very small, thus accounting for the extremely small conductance of the membrane in the resting steady state. When activator A is present, receptor sites bind A such that [AR′]/[AR] > [R′]/[R]. The resulting increase of forms AR′ plus R′ corresponding to the conducting state initiates the conductivity increase. The presence of the esterase insures rapid removal of the activator acetylcholine and thus quickly restores the initial closed state. The reaction scheme in Fig. 1 is analogous to others that have been formulated previously to describe the synaptic action of acetylcholine (see, for example, Colquhoun, 6). In 1957, del Castillo and Katz (7) introduced the explicit reaction scheme which is the upper path ($A + R \rightleftharpoons AR \rightleftharpoons AR'$) of the scheme shown in Fig. 1. As a general activator–receptor model, this scheme can be used successfully to model the transient Na^+ ion conductivity changes during excitation of axonal membranes (8–10).

In this article we discuss the functional implications of recent kinetic data on isolated acetylcholine receptors and acetylcholines-

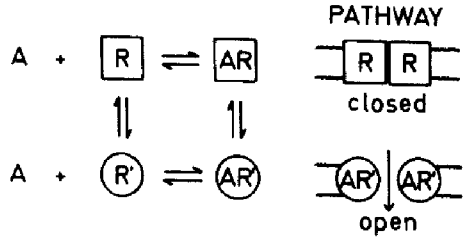

Fig. 1. Reaction scheme for the structural transition induced by acetylcholine A in the acetylcholine receptor binding sites: R, closed conformation and R′, open conformation. On the right is a schematic view of the receptor-mediated permeability change in the membrane.

terase obtained from the electric organs of electric fish. These organs are phylogenetically derived from muscle and provide excitable membranes rich in receptor and esterase which are thought to be closely analogous to mammalian excitable membranes. The kinetic differences between the two isolated proteins appear to complicate a molecular description of the close functional relationship between receptor and esterase indicated by electrophysiological data. We discuss various models and touch briefly several unsolved problems concerning acetylcholine-mediated information transfer.

II. LOCALIZATION OF ACETYLCHOLINE RECEPTOR AND ACETYLCHOLINESTERASE

Conditions required for the extraction of acetylcholine receptor and acetylcholinesterase from excitable membranes indicate that both proteins are predominantly membrane bound (11,12; also see Rosenberry, 13). Detergents are required for solubilization of the receptor, thus characterizing it as an integral protein of phospholipid membrane. Acetylcholinesterase is extracted from electric organ membranes at high ionic strength in the absence of detergent, although in several mammalian tissues the addition of detergent increases the amount solubilized (14,15). The esterase thus may be classified as a peripheral membrane protein, and recent evidence suggests that at synapses this enzyme is incorporated in the extracellular basement membrane matrix (16,17).

The histochemical localization of acetylcholinesterase in excitable membranes has long been established (see Koelle, 18,19,20) and is based on the deposition of esterase hydrolysis products by metal ion precipitation. A more quantitative measure of the concentration of active sites of receptor and esterase can be obtained by autoradiography with the use of radiolabeled ligands which bind to the active sites with virtual irreversibility. Autoradiographic studies of mouse sternomastoid neuromuscular junctions by Fertuck and Salpeter (21) with ^{125}I-labeled α-bungarotoxin suggest particularly high receptor concentrations in the juxtaneuronal postsynaptic membrane. Relatively few receptors appear to extend into the depths of the postsynaptic folds. Similar studies of acetylcholinesterase with [^{3}H]diisopropylfluorophosphate suggest a more uniform distribution along the synaptic membranes (22,23). It is noteworthy that the resolution of the autora-

diographs in these studies is not sufficient to specify the distribution of receptor and esterase between pre- and postsynaptic membranes (21). Electron microscopy involving either immunoperoxidase techniques (24) or peroxidase-labeled α-bungarotoxin (25) reveal both a postsynaptic and a presynaptic receptor localization. However, it is clear from the cited autoradiographic studies that the apparent membrane concentrations of receptor and esterase are much lower in extrajunctional regions than within the junction.

Several reports have indicated that the ratio of total active sites of receptor and esterase is about 1 both in electric organ and in muscle (26–29), although the ratio appears to increase after denervation of rat diaphragm (14,30). In rat diaphragm there are about 4×10^7 receptor sites per end plate (28,31) and about the same number of acetylcholinesterase sites (32), although the determination of acetylcholinesterase sites is uncertain by perhaps a factor of two because some diisopropylfluorophosphate-labeled sites may not correspond to acetylcholinesterase (32). If one assumes an exclusive and homogeneous postsynaptic localization, this number corresponds to about 10^4 sites/μm^2 (33). However, postsynaptic receptors do not appear to be distributed homogeneously, as noted in the preceding paragraph, and maximum receptor densities of 3×10^4 sites/μm^2 have been estimated for the juxtaneuronal postsynaptic membrane of mouse sternomastoid muscle (21). This estimate is quite close to that for receptor densities in the subsynaptic membrane of eel electroplax (34) and suggests very high membrane concentrations which approach maximum values calculated for close packing of receptors in the membrane (33).

As suggested by the morphological evidence, electrophysiological data reveal a close functional relationship between receptor and esterase in controlling the action of acetylcholine. Ionic currents in postsynaptic membrane were shown to be highly sensitive to inhibitors which blocked the access of acetylcholine to the active sites either of receptor or of esterase (35,36). More recently, Magleby and Stevens (37) presented evidence that the decay of end plate currents (epcs) in frog sartorius neuromuscular junction is longer than the estimated lifetime of the neurally evoked acetylcholine available to the receptors. The estimated time dependence of the free (unbound) acetylcholine concentration in their report was determined indirectly from the time course of the epcs and is indicated in line A of Fig. 2. Also shown as line B in Fig. 2 is the comparatively longer duration of miniature end plate currents (mepcs) is observed in toad neuromuscular

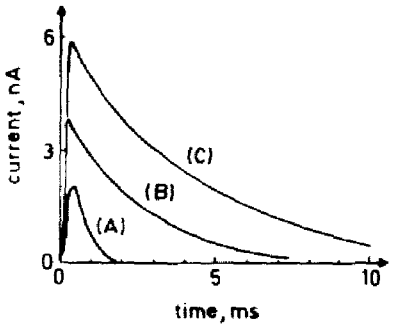

Fig. 2. Miniature end plate currents (mepcs; inward current positive) reflecting conductivity changes in a voltage-clamped toad muscle fiber at 22°C (redrawn from Gage and McBurney, 38); line B, in standard Ringer solution; line C, after incubating for 30 min in 1 mg/liter neostigmine. Line A represents the estimated concentration (in arbitrary units) of acetylcholine available to synaptic receptors following neural triggering of an end plate current (epc) (37). The similarity of the decay time constants and their voltage dependence for both epcs (37) and mepcs (38) justifies the application of epc estimates for acetylcholine to mepcs.

junctions by Gage and McBurney (38). The slow decay of the mepc in line B is exponential; and the time constant, voltage dependence, and temperature dependence of the decay is about the same as that observed for the decay of both neurally evoked epcs and acetylcholine-induced single channel openings by Stevens and his colleagues (37–39). The equivalence of these decay time constants supports the contention of Magleby and Stevens (37) that channel closing [or agonist dissociation (see Kordas, 40)] is rate limiting during epc (or mepc) decay such that free acetylcholine is no longer in equilibrium with the receptor.

In the presence of an acetylcholinesterase inhibitor, both the amplitude and the decay time of mepcs are increased by about 50%, as indicated in line C of Fig. 2, while the growth phase is virtually unaffected (38). Similar effects are seen with epcs (37,40,41). Thus esterase inhibition appears to result in activation of a greater number of receptors and an increase in the lifetime of free acetylcholine such that its removal from the cleft by diffusion contributes to the decay time constant (41). This diffusion appears to be slowed by the binding of acetylcholine to receptors, and addition of receptor inhibitors reduces receptor binding and restores the decay time constant to close to its original value in the absence of both esterase and receptor inhibitors (42). We may thus conclude that the effect of acetylcholinesterase inhibitors on epcs and mepcs particularly demonstrates the close functional as well as spatial proximity of receptor and esterase proteins.

III. DO RECEPTOR AND ESTERASE COMPETE FOR ACETYLCHOLINE?

In view of the close spatial and functional proximity of receptor and esterase, one may ask the question: Is the access of acetylcholine to these two proteins regulated in order to enhance their functionally sequential roles, such that acetylcholine first interacts with receptor and then with esterase? In the neurotransmitter theory of synaptic acetylcholine action (43), it is assumed that acetylcholine is released from the nerve terminal into the synaptic cleft. Receptor and esterase are then presumed to compete for the available acetylcholine, and it is evident that sufficient acetylcholine must bind to receptor to account for the observed conductance increase in the postsynaptic membrane. In the following sections we present recent kinetic data on the interaction of acetylcholine and its analogs with acetylcholine receptor and acetylcholinesterase. These studies suggest that, with the solubilized proteins from eel and torpedo electric organs, the esterase binds acetylcholine at least 10 times (and perhaps 100 times) more rapidly than the receptor. Such a difference appears to place the receptor at a considerable competitive disadvantage. We consider the implications of this disadvantage in a simple quantitative description of competitive acetylcholine action at the synapse. We also describe alternative models, including a sequential mechanism in which acetylcholine has access first to receptor and then to esterase. Such a sequential mechanism is included in a previous hypothesis of a partially intramembranous action of acetylcholine in excitable membranes (1–5,8–10).

IV. KINETIC ANALYSES

The presentation of our analyses of the interaction of acetylcholine (A) with receptor (R) and esterase (E) will focus on the reactions in Eqs. (1) and (2). Of particular relevance are the bimolecular reaction

$$A + R \underset{k_{-1}^R}{\overset{k_1^R}{\rightleftharpoons}} AR \tag{1}$$

$$A + E \underset{k_{-1}^E}{\overset{k_1^E}{\rightleftharpoons}} AE \tag{2}$$

rate constants k_1^R and k_1^E for acetylcholine binding to receptor and esterase, respectively. One might anticipate that both bimolecular reactions are close to diffusion controlled; that is, nearly every collisional

encounter between acetylcholine and an R or E binding site leads to binding. In practical terms this implies that the bimolecular reactions are very rapid (in the μsec or msec time range) and require special rapid kinetic methods. Furthermore, the analysis of rapid kinetic reactions is greatly facilitated when the reaction systems are homogeneous. Thus we have so far applied rapid kinetic techniques only to solubilized receptor or esterase of high purity.

A powerful method for the determination of rate constants of rapid chemical reactions is chemical relaxation spectrometry (44,45). The principle of this method is the perturbation of a chemical equilibrium or a steady-state by a rapid change in a physical variable, for example, temperature, followed by a measurement of a rate of concentration change as the components adjust to their new equilibrium or steady-state concentrations. Generally the concentration of one component is monitored by spectrophotometric or spectrofluorometric techniques. For small physical perturbations, the concentration change associated with a single elementary reaction such as those in Eqs. (1) and (2) has an exponential time dependence and is thus characterized by a relaxation time and a relaxation amplitude. A simple theoretical analysis (44) predicts that this relaxation time τ for the reaction in Eq. (1), for instance, will depend on the reactant concentrations according to Eq. (3),

$$\tau = [k_1^R([A] + [R]) + k_{-1}^R]^{-1} \tag{3}$$

where [A] and [R] are equilibrium concentrations. Usually [A] and/or [R] cannot be directly measured; and it is convenient to express Eq. (3) in terms of the total concentrations $[A^0]$ and $[R^0]$, where $[A^0] = [A] + [AR]$ and $[R^0] = [R] + [AR]$, as shown in Eq. (4) (see Winkler-Oswatitsch, 46).

$$\tau = [k_1^R[R^0]\sqrt{(1 + p + [A^0]/[R^0])^2 - 4[A^0][R^0]}]^{-1} \tag{4}$$

In Eq. (4) $p = K/[R^0]$ and $K = k_{-1}^R/k_1^R$. Equation (4) is readily rearranged to Eq. (5) (see Rosenberry and Neumann, 47).

$$\tau^{-2} = \alpha + \beta[A^0] + \alpha[A^0]^2 \tag{5}$$

where $\alpha = (k_1^R)^2(K + [R^0])^2$, $\beta = 2(k_1^R)^2(K - [R^0])$, and $\gamma = (k_1^R)^2$. Equations 4 and 5 have been written with apparent asymmetry of $[A^0]$ and $[R^0]$ in anticipation of experimental measurements of τ in which $[R^0]$ is constant while $[A^0]$ is varied. Under these conditions it is readily shown that τ has a maximum value (τ^{-2} a minimum) when $[A^0] = [R^0] - K$ provided that $[R^0] > K$, i.e., $p < 1$ [see Winkler-Oswatitsch (46) and Neumann and Chang (48)].

While measurement of the reaction rate constants of acetylcholine with receptor and esterase defined in Eqs. (1) and (2) by means of Eqs. (4) and (5) thus would appear straightforward, direct measurements have not yet been possible. In the receptor case, no suitable optical signal for monitoring the reaction in Eq. (1) itself has been found. However, this reaction can be coupled to Ca^{2+}-binding equilibria involving the receptor (48,49). Recently, multiple relaxations in this coupled system have been observed, and corresponding extensions of Eq. (4) permitted estimates both of several rate constants including k_1^R in Eq. (1) and of receptor site normalities (48,49; see Section VI). In the esterase case, the complex AE in Eq. (2) is an intermediate which can also react along a hydrolytic pathway with such speed that equilibrium relaxation measurements are not possible [see Eq. (6)]. However, a minimum estimate of k_1^E in Eq. (2) is available from steady-state kinetic data (see Section V).

For both receptor and esterase, the relaxation kinetics of specific fluorescent ligand binding at the active site have been studied (47,50). The fluorescent ligands used in these studies are shown in Fig. 3. They are highly fluorescent when free in solution but totally quenched on binding to the active site, and this difference in fluorescence intensity allows monitoring of concentration changes during temperature-jump relaxation studies. These ligands appear to act as specific analogs of acetylcholine and have provided valuable information about bimolecular reaction rate constants for both proteins, which is discussed in the following sections.

V. ACETYLCHOLINESTERASE

A. STRUCTURE

Several forms of the esterase, characterized by sedimentation coefficients of 18 S, 14 S, 8 S, and 11 S, have been purified from eel electric organ extracts by affinity chromatography (13,17). Electron microscopic (51,52) and biochemical (16,17) studies indicate that the 18 S, 14 S, and 8 S species correspond, respectively, to 3, 2, and 1 catalytic subunit tetramers attached to a 50 nm collagenlike tail structure by disulfide bonds. The 11 S form corresponds to a single catalytic subunit tetramer devoid of the tail structure. Esterase at rat diaphragm end plates appears to have a similar tail structure (14). The tail structure has little effect on the catalytic activity (53) but has been suggested to be responsible for the esterase membrane attachment (11,16). Acetylcholinesterase at synapses may be localized in the extracellular basement membrane (11,16,54,55).

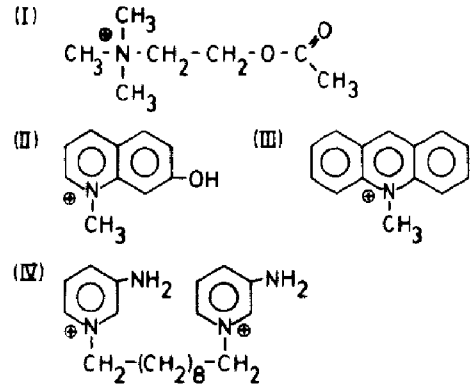

Fig. 3. Chemical formula of acetylcholine (I), 1-methyl-7-hydroxyquinolinium (II), *N*-methylacridinium (III), and bis(3-aminopyridinium)-1, 10-decane (IV).

B. STEADY-STATE KINETICS

Numerous studies have demonstrated that a minimal mechanism for the hydrolysis of acetylcholine by acetylcholinesterase is given by the reaction in Eq. (6) (see Rosenberry, 13).

$$A + E \underset{k_{-1}^E}{\overset{k_1^E}{\rightleftharpoons}} AE \xrightarrow{k_2} \underset{\text{choline}}{\text{acetyl E}} \xrightarrow{k_3} \underset{H_2O}{E + \text{acetate} + H^+} \tag{6}$$

Under steady-state conditions ($[A] \gg [E^0]$), the velocity (v) of the acetylcholine hydrolysis is given by Eq. (7).

$$v = \frac{k_{cat}[E^0]}{1 + K_{app}/[A]} \tag{7}$$

where $k_{cat} = k_2k_3/(k_2 + k_3)$ and $K_{app} = k_{cat}(k_{-1}^E + k_2)/k_1^E k_2$. At high acetylcholine concentrations ($[A] > K_{app} \cong 10^{-4}\ M$), v becomes first order in $[E^0]$; and values of the first-order rate constant $k_{cat} = 1.6 \times 10^4\ sec^{-1}$ (0.1 M ionic strength, pH 8.0, 25°C) have consistently been measured (see Rosenberry, 13). The relevance of this extremely high rate constant to acetylcholine-mediated neuronal information transfer was first recognized by Nachmansohn (56a). With acetylcholine as substrate, k_{cat} is thought to approximate k_3 (13), and k_2 has been estimated to be about $10^5\ sec^{-1}$ (56). At low acetylcholine concentrations v becomes second order, and the second-order rate constant k_{cat}/k_{app} has been measured as $1.6 \times 10^8\ M^{-1}sec^{-1}$ under the same experimental conditions (13). According to Eq. (6), the second order rate constant is given by Eq. (8),

$$\frac{k_{cat}}{K_{app}} = k_1^E\left(\frac{k_2}{k_{-1}^E + k_2}\right) \tag{8}$$

and thus it is apparent that k_{cat}/K_{app} establishes a minimum value for k_1^E. Detailed kinetic studies suggest that the actual esterase mechanism is somewhat more complicated than that in Eq. (6) (57). Even in this more complicated mechanism, however, k_{cat}/K_{app} would still underestimate k_1^E.

At very high acetylcholine concentrations ($\geq 10^{-2}$ *M*) substrate inhibition of acetylcholine hydrolysis may be detected (see Augustinsson, 58). While some controversy about the mechanism of substrate inhibition exists (59), strong evidence indicates that this inhibition arises from the binding of acetylcholine to the active site in the *acetylenzyme* with consequent inhibition of deacylation (60,61).

C. RELAXATION KINETICS

Two cationic ligands which have been used in temperature jump studies of acetylcholinesterase are *N*-methylacridinium and 1-methyl-7-hydroxyquinolinium (47; see Fig. 3). Both ligands bind with high specificity to the esterase active site. The interaction of *N*-methylacridinium with acetylcholinesterase was analyzed according to Eq. (5) and is shown in Fig. 4. Bimolecular reaction rate constants and equilibrium dissociation constants for both ligands are given in Table I. The observed bimolecular reaction rate constants of some-

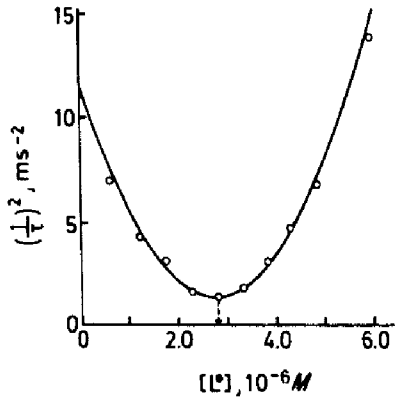

Fig. 4. Dependence of the mean values of the relaxation times, τ, observed with acetylcholinesterase and *N*-methylacridinium on total ligand concentration, [L°], in 0.1 *M* sodium phosphate at pH 8.0 and 23°C (47). Initial concentration of esterase active sites [E°] = 2.92×10^{-6} *M*. Data are plotted according to Eq. (5). The solid line was calculated from a weighted least-squares analysis based on a second-order polynomial in [L°]. From the position of the minimum, the value of $[E^\circ] = [L^\circ]_{min} - K = 2.94(\pm 0.04) \times 10^{-6}$ *M* can be obtained independently from the kinetic titration; it is consistently the same as the initial concentration of esterase sites determined by thermodynamic techniques.

TABLE I
Equilibrium Dissociation Constants K and Rate Constants for the Interaction of Acetylcholinesterase and Cationic Ligands [Eq. (2)][a]

Compound[b]	k_1^E (M^{-1} sec^{-1})	K (M)	k_{-1}^E (sec^{-1})
(I)	$\geq 1.6 (\pm 0.1) \times 10^8$		
(II)	$2.18 (\pm 0.15) \times 10^9$	$2.03 (\pm 0.3) \times 10^{-7}$	4.4×10^2
(III)	$1.18 (\pm 0.03) \times 10^9$	$1.49 (\pm 0.03) \times 10^{-7}$	1.8×10^2

[a] From Rosenberry and Neumann (47).

[b] (I), Acetylcholine in 0.1 M ionic strength at 25°C, pH 8.0; (II), 1-Methyl-7-hydroxyquinolinium in 0.1 M sodium phosphate at 23°C, pH 7.0; (III), N-methylacridinium in 0.1 M sodium phosphate at 23°C, pH 8.0.

what greater than $10^9\ M^{-1}$ sec^{-1} are unusually high for enzyme–ligand interactions (see Rosenberry and Neumann, 47). Recent data show a very high ionic strength dependence of k_1^E for these fluorescent ligands consistent with an "effective" negative charge on the enzyme active site of about −6 (62). Virtually the same ionic strength dependence is observed for k_{cat}/K_{app} for acetylthiocholine [see Eq. (8)], a substrate whose structure and kinetic properties are very similar to those of acetylcholine. Thus k_1^E values for several cationic ligands, including acetylcholine, appear to be unusually high because of the large electrostatic interaction between ligand and esterase. Several fixed negative charges near the active site may contribute to the high effective negative charge on the esterase, thereby creating a "binding surface," involved in trapping acetylcholine, that is considerably larger than the catalytic site itself.

VI. ACETYLCHOLINE RECEPTOR

A. STRUCTURE

While isolation of the various electric organ acetylcholinesterase species poses no major problems, the purification of native acetylcholine receptor is still a difficult task. Conventional homogenization procedures may result in chemical modification of the receptor even prior to its extraction from the membrane, as the following observations suggest. Solubilized receptor purified from torpedo electric organ exists in two major forms (63): a heavy (H) form (13 S) and a light (L)

form (9 S). It has been recently established that the H form is a dimer of L forms linked by an intermolecular disulfide bond involving the 67,000-dalton subunits of the receptor and that, without precautions, the apparently native dimeric H form is split by disulfide reduction into monomeric L forms during homogenization of torpedo electric organ (64). This cleavage may be prevented by homogenization in the presence of *N*-ethylmaleimide, a sulfhydryl alkylating agent. In crude extracts, the receptor H form appears to bind acetylcholine more tightly than the L form, the respective equilibrium dissociation constants (K_d) being $(3 \pm 1) \times 10^{-9}\,M$ and $(2 \pm 1) \times 10^{-8}\,M$. After purification of the H or L forms by affinity chromatography, however, the binding affinity of acetylcholine to either form is partially converted to a lower value ($K_d \cong 10^{-6}\,M$) (64). The conversion of H to L forms by endogenous reducing agents as well as these variations in acetylcholine affinities serve to remind us that, in general, extrapolation of protein properties in solution to those *in vivo* should be done with caution.

B. Ca^{2+}-BINDING PROPERTIES

Detergent-solubilized isolated receptor binds large amounts of Ca^{2+} ions (49,65). The Ca^{2+} binding isotherm shows two extended linear regions in Scatchard plots, suggesting at least two types of independent Ca^{2+} binding sites (49). Data on the stoichiometry and affinity of Ca^{2+} binding are summarized in Table II. As noted in Section I, Nachmansohn has proposed that the binding of acetylcholine to the receptor causes the release of receptor-bound Ca^{2+} ions (4). A recent test of this proposal has demonstrated that isolated receptor does indeed

TABLE II
Apparent Equilibrium Dissociation Constants K_{Ca} and Maximum Number B^0 of Ca Binding Sites per 380,000 (±20,000) Daltons of the Isolated Acetylcholine Receptor from *Torpedo californica* in 0.1 *M* NaCl, 0.05 *M* Tris HCl, 0.1% Brij, pH 8.5 at 20°C[a,b]

Region	K_{Ca} (M)	B^0
(1)	$3.3\ (\pm 0.3) \times 10^{-4}$	44 (± 4)
(2)	$\leq 2.5\ (\pm 0.5) \times 10^{-6}$	34 (± 4)

[a] From Chang and Neumann (49).

[b] The data were obtained from a Scatchard plot where two extended linear regions suggest at least two types of independent Ca^{2+} binding sites. The overall acetylcholine equilibrium constant of the receptor preparation was $10^{-6}\,M$.

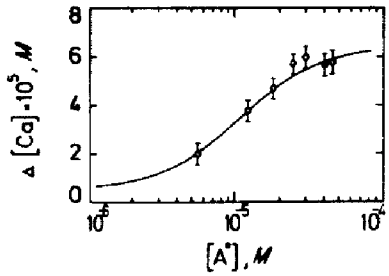

Fig. 5. The change in concentration of free Ca^{2+} ions reflecting release of bound Ca^{2+}, Ca_b^{2+} ($\Delta[Ca^{2+}] = -\Delta[Ca_b^{2+}]$), from isolated acetylcholine receptor of *Torpedo californica* (in 0.1 *M* NaCl, 0.05 *M* Tris HCl, 0.1% Brij, 0.00 12 *M* Ca, pH 8.5, at 20°C) as a function of the total acetylcholine concentration [A^0] (49). The receptor concentration is 2.6 mg/ml.

release Ca^{2+} ions upon binding acetylcholine (48,49). As shown in Fig. 5 there is progressive release of Ca^{2+} ions from the receptor on addition of acetylcholine until an apparent saturation level is reached. The Ca^{2+} release curves can be quantitatively analyzed in terms of the overall reaction in Eq. (9)

$$nA + RCa_x \rightleftharpoons A_nR + xCa \tag{9}$$

where $n = 2$ is the number of acetylcholine ions bound to the receptor (H form), x is the maximum number of Ca^{2+} ions which can be released by acetylcholine binding, and A_nR represents the receptor conformations with bound acetylcholine. The analysis indicates that at 1.2 m*M* [Ca^{2+}], $x = 5$ (± 1); in other words, two to three Ca^{2+} ions are released per bound acetylcholine. Furthermore, subsequent addition of α-bungarotoxin to the receptor solutions displaces the bound acetylcholine and leads to reuptake of the Ca^{2+} ions originally released. It thus seems that receptor activators and inhibitors have opposing effects on the Ca^{2+} binding of receptors (49).

C. RELAXATION KINETICS

As noted in Section IV, no direct method of rapidly monitoring acetylcholine reactions with the isolated receptor is currently available. Therefore, the binding of acetylcholine has been analyzed by its coupling with Ca^{2+} release from the receptor (48). The kinetic data suggest that the receptor is equilibrated among at least three conformations ($R \rightleftharpoons R'' \rightleftharpoons R'''$). When acetylcholine is present, at least two of these states contribute in a characteristic manner to the chemical relaxation spectrum. It appears that the main reaction path for the interaction with acetylcholine is $A + R \rightleftharpoons AR \rightleftharpoons AR''$, indicating at least one intramolecular (conformational) change influenced by the bind-

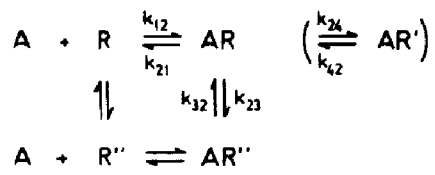

Fig. 6. Reaction scheme for the interaction of acetylcholine with isolated receptor from *Torpedo californica*, suggested by kinetic studies in which the release of Ca^{2+} ions is used as an indicator for acetylcholine binding. The observed main reaction path is A + R ⇌ AR ⇌ AR″, with [R″] ≪ [R]. The AR ⇌ AR″ relaxation is slow and well separated from the initial binding step. The bimolecular rate constant k_{on} is k_{12} [equivalent to k_1^R in Eq. (1)]; the dissociation rate constant k_{off} is k_{21} [equivalent to k_{-1}^R in Eq. (1)] or, if a step AR ⇌ AR′ is rapidly coupled to the observed bimolecular reaction, $k_{off} = k_{21}k_{42}(k_{42} + k_{42})^{-1}$(see Neumann and Chang, 48).

ing of activator. This reaction path is included in a reaction scheme suggested by the relaxation kinetic data in Fig. 6. Within the experimental accuracy there was no evidence for cooperativity between the two acetylcholine binding sites in the receptor macromolecule, and thus this scheme is simply expressed in terms of binding sites. Data from the relaxation kinetic studies are summarized in Table III.

Although the schemes dipicted in Figs. 1 and 6 are formally quite similar, the time range calculated for the reaction step AR ⇌ AR″ in Fig. 6 is 20 to 50 msec and thus falls outside the physiologically relevant domain of 1 to 10 msec observed for the relaxation times of receptor-mediated conductivity changes (66) modeled by the scheme in Fig. 1. Since the kinetic data on isolated acetylcholine receptor do not exclude the presence of a rapidly coupled structural transition AR ⇌ AR′ (see Appendix), this step is included in Fig. 6 to model the channel activation in the scheme shown in Fig. 1.

It is apparent from Table III that the rate constant $k_1^R = 2.4 \times 10^7$ M^{-1} sec^{-1} for the association of acetylcholine to receptor is relatively

TABLE III

Kinetic and Thermodynamic Parameters of the Interaction of Acetylcholine with Isolated Acetylcholine Receptor from *Torpedo californica*, for the Main Reaction Path A + R ⇌ AR ⇌ AR″ [a,b]

A + R ⇌ AR	AR ⇌ AR″
$k_{on} = 2.4\ (\pm 0.5) \times 10^7\ M^{-1}\ sec^{-1}$	$k_{23} = 43.5\ sec^{-1}$
$k_{off} = 140\ sec^{-1}$	$k_{32} = 6.5\ sec^{-1}$
$K_1 = 0.6 \times 10^{-5}\ M$	$K_2 = 6.7$

[a] From Neumann and Chang (48).

[b] The solvent is composed of 0.1 *M* NaCl, 0.1% Brij, 0.001 *M* Ca, 0.05 *M* Tris HCl, pH 8.5, at 23°C. The overall acetylcholine equilibrium constant $\overline{K} = K_1(1 + K_2)^{-1}$ was 10^{-6} *M*, where $K_1 = k_{off}/k_{on}$ and $K_2 = k_{23}/k_{32}$.

low compared to k_1^E values. It is noteworthy that recent stopped-flow experiments involving receptor-rich membrane fragments of *Torpedo marmorata* and the dication suberyldicholine have yielded a bimolecular rate constant of $1.0 \times 10^7\ M^{-1}\ sec^{-1}$ (F. Barrantes, personal communication), comparable to the rate constant k_1^R for the binding of acetylcholine to isolated receptor in Table III. On the other hand, recent relaxation kinetic experiments with the dicationic inhibitor bis(3-aminopyridinium)-1, 10-decane (DAP) (see Fig. 3), and the isolated receptor from *Torpedo marmorata* have shown that this ligand has a bimolecular rate constant of $\sim 10^8\ M^{-1}\ sec^{-1}$ (0.1 *M* ionic strength, pH 7.0, 20°C). The ionic strength dependence of the association rate constant for DAP suggests an "effective charge" of $-3\ (\pm 1)$ on the binding site of the protein. This value is somewhat less negative than that indicated for the acetylcholinesterase active site. However, it seems that in both proteins there are large electrostatic contributions to the rate with which cationic ligands like acetylcholine are bound.

Independent information about acetylcholine interactions with *in vivo* receptor has recently been obtained from electrophysiological experiments by Sheridan and Lester (66). Applying voltage-jump perturbations, postsynaptic current relaxation times in eel electroplax could be evaluated as a function of the steady-state concentration of externally applied acetylcholine. Within the limited concentration range of 10^{-5} to $10^{-4}\ M$, the relaxation times of the measured currents appeared to be bimolecularly controlled by acetylcholine; and the bimolecular rate constant was estimated to be $10^7\ M^{-1}\ sec^{-1}$. The apparent dissociation rate constant was strongly dependent on clamp voltage and spanned the range from 10^2 to $10^3\ sec^{-1}$. These values are comparable to the rate constants obtained for the isolated receptor. In particular, the similarity between the values of $k_{on} = 10^7\ M^{-1}\ sec^{-1}$ from current relaxations and $k_1^R = 2.4 \times 10^7\ M^{-1}\ sec^{-1}$ from kinetic studies on isolated receptor suggests that the rate of coupled Ca^{2+} release not only reflects the rate of acetylcholine binding to isolated receptor, but also may represent the rate-limiting step for the conductivity increase in the membrane.

A second important indication from this electrophysiological study arose from the dependence of the relaxation current amplitude on acetylcholine concentration. The current data suggested that at least two acetylcholine molecules must bind to receptor to open a single channel conductance unit (66). This suggestion that the active receptor unit is dimeric may be related to the fact that the H form of detergent-solubilized receptor binds two acetylcholine molecules.

The stoichiometry of the acetylcholine binding and the various re-

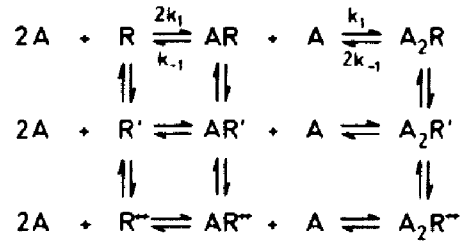

Fig. 7. Reaction scheme for the interaction of acetylcholine with *in vivo* receptor as suggested by electrophysiological studies. The three receptor states correspond to the R (closed), R′ (open), and R^{++} (desensitized) states. The acetylcholine binding sites are assumed to be equivalent and independent, as indicated by the rate coefficients k_1 and k_{-1} with their appropriate statistical factors.

ceptor states indicated by electrophysiological studies may be summarized in the general reaction scheme depicted in Fig. 7. In this scheme the association–dissociation steps are represented horizontally and the conformational transitions between three receptor states are given vertically. These three states correspond to the R (closed), R′ (open), and R^{++} (desensitized) states. The desensitized state is an inactive receptor form which can be detected in the continued presence of externally applied acetylcholine (67). Under *in vivo* conditions it appears that $[R'] + [R^{++}] \ll [R]$. Thus, under various experimental conditions, only a few of all the possible reactions depicted in the scheme in Fig. 7 may contribute to a measurable extent to the observed phenomena. For instance, neurally triggered receptor activation does not lead to desensitization; thus the state R^{++} seems uninvolved in the determination of neurally triggered epc's.

VII. COMPARISONS BETWEEN COMPETITIVE AND SEQUENTIAL REACTIONS OF ACETYLCHOLINE AT THE SYNAPSE

The electrophysiological characteristics of impulse transmission at neuromuscular junctions establish, as we noted in Section II, a close functional relationship between receptor and esterase which is probably based on a close spatial proximity of these two proteins. We now wish to incorporate the kinetic data presented on the interactions between acetylcholine and these proteins after isolation with the structural localization of the proteins in the synapse. Predictions of the rates and extents of acetylcholine interactions thus can be made and compared with the electrophysiological data. This task is complicated by the assumptions necessary for a quantitative analysis. The foremost assumption is that rate constants obtained with the isolated

proteins in solution are applicable to the membrane-bound proteins in the synapse. The rate constants of greatest interest here, the bimolecular association constants for acetylcholine, probably satisfy this assumption rather well, although additional electrostatic contributions by the membrane environment and an altered acetylcholine diffusion rate in the synaptic gap are possible sources of alterations. The close correspondence of k_1^R from the kinetic (48) and electrophysiological (66) studies noted above support the use of this assumption. The second assumption involves an approximation of the geometry, topology, and homogeneity of the reaction space within the synapse. This approximation may involve local concentration gradients either of the proteins or of acetylcholine. Two alternatives regarding the homogeneity of the reaction space are the competitive versus the sequential modes of acetylcholine interaction noted in Section III. We consider these two alternative modes in the following sections with full awareness of the reaction space approximations required.

A. COMPETITION MODELS

Localization data in Section II indicate 4×10^7 receptor sites for α-neurotoxin per rat diaphragm end plate and nearly an equal number of esterase sites. Furthermore, there appears to be two toxin sites per acetylcholine site on the receptor (64). Direct measurements of acetylcholine release from esterase-inhibited rat diaphragm end plates during nerve stimulation lead to estimates of 3 to 6×10^6 acetylcholine molecules released per end plate potential (68,69). For the calculations that follow we assume simply that both the proteins and acetylcholine are homogeneously distributed. This homogeneous reaction space assumption prohibits concentration gradients over the duration of the end plate potential. It thus does not consider the proposal of acetylcholine release from spatially discrete resides; the possibility of acetylcholine diffusion from the synaptic cleft; and any inhomogeneity in receptor or esterase distributions. We also assume acetylcholine release is essentially instantaneous. This assumption is not very good for epcs (70) but is probably much better for the mepcs shown in Fig. 2. These two assumptions reduce the kinetic description of epcs to the chemical reactions in Fig. 1 and Eq. (6). A quantitative solution to the differential equations arising from this kinetic description is given in the Appendix. The solution is greatly simplified by noting that, within the homogeneous reaction space assumption, the concentrations of both receptor and esterase active sites are about fivefold in excess of the total initial acetylcholine concentration. Under this con-

dition, the free active site concentrations are approximately given by the total active site concentrations: $[R] \cong [R^0]$ and $[E] \cong [E^0]$. Several important features of the Appendix solution become apparent by considering the association fluxes J of the receptor and esterase reactions with acetylcholine in Eqs. (1 and 2). When the dissociation fluxes are negligible, these fluxes are sufficient to account for the distribution of acetylcholine between receptor and enzyme, as shown in Eqs. (10 and 11).

$$J^R \equiv k_1^R[A][R] \cong k_1^R[A][R^0] \cong \frac{d[AR]}{dt} \tag{10}$$

$$J^E \equiv k_1^E[A][E] \cong k_1^E[A][E^0] \cong \frac{d[AE]}{dt} \tag{11}$$

Integration under the initial condition that at $t = 0$, $[A] = [A^0]$ leads to Eq. (12).

$$\frac{[AR]}{[A^0]} = \frac{k_1^R[R^0]}{(k_1^R[R^0] + k_1^E[E^0])} \{1 - \exp[-k_1^R[R^0] + (k_1^E[E^0])t]\} \tag{12}$$

With values of $k_1^R = 2 \times 10^7 M^{-1}\,\text{sec}^{-1}$ and $k_1^E = 2 \times 10^8 M^{-1}\,\text{sec}^{-1}$ given in Sections V and VI, together with the condition $[R^0] = [E^0]$, the maximum value of $[AR]/[A^0]$ obtained from Eq. (12) is 0.1. The more extensive treatment in the Appendix gives a similar $[AR']_{max}/[A^0]$ value of 0.082. If one AR′ corresponds to one open ion channel, then this $[AR']_{max}/[A^0]$ ratio indicates that somewhat less than 10% of the total released acetylcholine activates about 1% of the total receptors (recall $[R^0] \cong 5[A^0]$ during an epc, in reasonable agreement with values estimated electrophysiologically from epc peak amplitudes (see Colquhoun, 6). If, however, as recent electrophysiological data (66) summarized in Fig. 7 suggest, only a dimeric A_2R' corresponds to one open channel and if acetylcholine binding at both sites is characterized by the k_1^R given above, then $[A_2R']_{max}/[R^0] \leq 10^{-4}$ [note that $[A_2R']/[R^0] = \frac{1}{2}[AR']/[R^0]^2$, see Eq. (A15)]. This is a 100-fold lower value than the electrophysiological estimate. In fact, to achieve an activation of 1% of the total receptors from dimeric A_2R' within the homogeneous reaction space assumption, nearly all the released acetylcholine would have to react with receptor before it reacted with esterase.

Because J^E is considerably larger than J^R, Eq. (12) also predicts that the epc peak amplitudes as well as the epc growth times should be quite sensitive to esterase inhibitors. When Eq. (12) is extended to include the dissociation fluxes in Eqs. (1 and 2), 99% esterase inhibition is predicted to increase the epc peak amplitudes by a factor of 8.1 in a

monomeric receptor scheme (Fig. 1) and by a factor of 65 in a dimeric receptor scheme (Fig. 7) and to increase the time to peak amplitude from about 220 μsec to 2.0 msec in either model (see Appendix). In contrast, the observed growth times for mepc's in Fig. 2 are virtually unaffected by esterase inhibition and peak amplitudes are increased only about 50%. Only slightly larger esterase inhibition effects are seen on epc's (71).

Despite the fact that the numerical estimates can be altered somewhat by assuming some variation in $[R^0]/[E^0]$ ratios, these comparisons lead us to conclude that the competition model with the homogeneous reaction space assumption is probably inappropriate for a monomeric receptor scheme and certainly inappropriate for a dimeric receptor scheme when the entire duration of the epc is being simulated. This model may be appropriate for the kinetics of the epc decay phase (see Magleby and Stevens, 37) under conditions in which acetylcholine diffusion from the synaptic cleft is not of major significance. In this respect it is noteworthy that the model predicts that 90% esterase inhibition would increase the decay rate constant by a factor of only two (see Appendix), a value consistent with electrophysiological observations (37).

One may consider alternatives to the homogeneous reaction space assumption in either competitive or sequential models. A quantitative treatment of these alternatives is beyond the scope of this chapter, but features which overcome shortcomings inherent in the homogeneous reaction space assumption can be noted.

An important alternative competitive model involves the assumption of a spatially nonhomogeneous acetylcholine concentration. This assumption applies to a vesicular release of acetylcholine, as currently proposed in the neurotransmitter theory (43). One may assume, for example, that acetylcholine released at the endplate by nerve stimulation is initially confined to volume elements corresponding to only 1% of the total potential reaction space. If receptor and esterase remain homogeneously distributed in the reaction space, then the initial acetylcholine concentration in these volume elements is twentyfold in excess of the total receptor or esterase concentrations. Under these conditions local saturation of receptor and enzyme would quickly occur (the time to half-saturation of receptors would be of the order of 30 μsec and of the esterase, about 3 μsec) but would be counterbalanced by acetylcholine dilution arising from diffusion into the entire reaction space. Model calculations thus must consider both diffusion and chemical reactions. While this model qualitatively would appear to result in a more favorable competition of receptor for acetylcholine than

in the homogeneous reaction space model above (i.e., a greater $[AR']_{max}/[A^0]$), the quantitative predictions of such a model are not evident simply by inspection.

B. SEQUENTIAL MODELS

Sequential processing of acetylcholine can occur if receptor and esterase are topologically arranged such that the receptor sites for the acetylcholine binding are closer to the sites of neurally triggered acetylcholine release. Such a nonhomogeneous protein distribution is involved in a spatial separation model, which proposes receptors clustered in the juxtaneuronal part of postsynaptic membranes and esterase distributed uniformly within the synaptic cleft (21,33). This spatial separation model also would suggest greater acetylcholine binding to receptor than in the homogeneous reaction space model but may conflict with the close coupling of receptor and esterase indicated by electrophysiological data. A quantitative treatment of this model is hampered by the lack of structural details on the exact localization of esterase relative to the receptor.

Quite a different line of thinking is involved in a *translocation* model for acetylcholine processing (9,72). This approach is based on a general acetylcholine theory of nerve excitation originally proposed and developed by Nachmansohn (1–5; see article by Nachmansohn in this volume). According to this model the reactions of acetylcholine with receptor and esterase are strictly organized, and close proximity of both proteins is assumed. Recently, explicit separation of the total reaction space into "microreaction spaces" has been introduced into the model (8,9). According to this concept, acetylcholine released by a nerve impulse first has access to receptor in a reaction space 1. The structural transition in the initial receptor–acetylcholine complex induced by acetylcholine binding translocates the bound acetylcholine ion to another reaction space 2 where acetylcholine dissociates and esterase activity prevents the return of acetylcholine to the receptor. Esterase activity is restricted to reaction space 2 and is thus an integral part of this sequential mechanism, insuring practically unidirectional flow of acetylcholine through the receptor system. This nonequilibrium aspect of the translocation model may be summarized in the flow scheme with separated reaction spaces shown in Fig. 8. The model may be applied both to conduction along excitable membranes and to transmission at the synapse (1–5, 8–10). At the synapse, presynaptic nerve stimulation causes a transient increase of K^+ ions in the synaptic gap. Since the postsynaptic membrane potential is sensitive to K^+, such an increase must lead to a potential

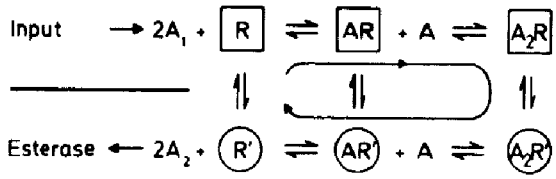

Fig. 8. Flow scheme for neurally triggered acetylcholine (input) in the sequential translocation model. The curved arrow indicates the flow of acetylcholine A_1 from a reaction space 1 through the closed (R) and open (R') receptor states to reaction space 2 where also esterase has access to acetylcholine A_2.

change in the postsynaptic membrane. It is this change of membrane potential which has been proposed to induce a transient increase in the acetylcholine concentration in the (probably intramembraneous) reaction space 1 and thus to amplify the flow of acetylcholine along the reaction path $R \rightarrow A_2R \rightarrow A_2R' \rightarrow R$ (see curved arrow in Fig. 7). An essential role of K^+ ions at synapses is also emphasized by von Euler (see article by von Euler in this volume). Acetylcholine, once translocated into the (probably extramembranous) reaction space 2, is exposed to virtually irreversible hydrolysis by the esterase. Thus neural activity drives the schematic "receptor cycle" essentially clockwise in one direction. The postulated separation of receptor and esterase reactions insures optimal use of available acetylcholine and avoids problems arising from the slower association of acetylcholine with the receptor than with the esterase. The sequential character of the flow scheme would also account for the observation that the growth time of miniature end plate currents is independent of esterase inhibition (see Fig. 2). Finally, if the acetylcholine reaction with the receptor in reaction space 1 occurs intramembranously, locally high concentrations of acetylcholine should lead to local receptor saturation. However, as mentioned in the discussion of the various other models for the *in vivo* association of acetylcholine with receptor and esterase, a quantitative analysis of the translocation model must await the elucidation of further organizational and functional details of the receptor and esterase system.

Other unresolved problems of acetylcholine-mediated neuronal information transfer include the relevance of the phenomenon of pharmacological desensitization (67) and the functional role of presynaptic and extrasynaptic receptor and esterase. The neurotransmitter theory does not explicitly consider pre- and extrasynaptic cholinergic proteins; and the vesicle hypothesis, modeling synaptic vesicles as the exclusive source of acetylcholine released during excitation, does not incorporate the observation of nonpostsynaptic acetylcholine receptors. On the other hand, the postulate of an intramembranous processing of acetylcholine by receptors in all excitable membranes

offers a functional role also for pre- and extrajunctional and axonal receptors (1–5).

While the quantitative estimates from the homogeneous reaction space assumption discussed above have suggested that the reaction space at the synapse is nonhomogeneous, there is currently no unequivocal evidence to differentiate between any of the alternative competitive or sequential models proposed. Thus the close functional relationship between receptor and esterase and the coupling of acetylcholine reactions to membrane permeability changes remain objects for experimental and theoretical studies.

APPENDIX: QUANTITATIVE SIMULATION OF NEURALLY EVOKED END PLATE CURRENTS ASSUMING A HOMOGENEOUS REACTION SPACE*

The general solutions to the differential equations arising from the receptor reaction scheme in Fig. 1 and the esterase reaction mechanism in Eq. (6) are too complex to be useful in this analysis. Simplifications and conditions introduced in Section VII will be assumed here: a homogeneous reaction space at the synapse; and the total concentrations $[R^0] \cong]E^0] \cong 5[A^0]$ estimated at a rat diaphragm end plate during a neurally triggered end plate current (epc). It follows that $[R] \cong [R^0]$ and $[E] \cong [E^0]$ during the entire duration of the epc (see Section VII). Additional simplifications in the chemical reaction schemes are indicated in the following paragraphs.

Electrophysiological data suggest that perturbations of receptor–acetylcholine equilibria in the end plate (e.g., by voltage-jump) result in epc relaxations that are characterized by a single exponential time course (66), and temperature-jump kinetic studies involving isolated receptor and acetylcholine show single exponential relaxations in the time range which corresponds to *in vivo* epcs (48). These observations suggest that the scheme of Fig. 1 can be reduced to the overall reaction shown in Eq. (A1).

$$A + R \underset{k_{-1}^{R*}}{\overset{k_1^{R*}}{\rightleftharpoons}} AR' \qquad \text{(A1)}$$

In Eq. (A1), k_1^{R*} and k_{-1}^{R*} are observed composite rate constants containing rate constant terms from each reaction in Fig. 1. This reduction of the scheme in Fig. 1 can arise from several alternative physical situ-

* By T. L. Rosenberry.

ations. Examples include the case in which species R′ is negligible as a reaction partner and the equilibrium AR ⇌ AR′ is rapid; and the case in which R′ and AR are present only at low concentration in a steady-state and R′ makes only a small contribution as a reaction partner. A situation assumed in other treatments (37,66), that R′ is negligible and A + R ⇌ AR is rapid, could be modeled by an extension of the following calculations and would explicitly require the value of the rapid equilibrium dissociation constant.

Reduction of the acetylcholinesterase mechanism in Eq. (6) to that in Eq. (A2) follows simply from the stipulation that [E] ≅ [E^0].

$$\mathrm{A} + \mathrm{E} \underset{k_{-1}^{E}}{\overset{k_1^{E}}{\rightleftharpoons}} \mathrm{AE} \xrightarrow{k_2} \text{acetyl E} \tag{A2}$$

Because [E] is not determined by the extent of acetyl enzyme formation or by the rate of its hydrolysis, the deacetylation portion of the mechanism [k_3 in Eq. (6)] does not effect the time course of acetylcholine removal. This would eliminate, for example, any effect of substrate inhibition of deacetylation on the simulation of epcs below. The reaction in Eq. (A2) can be further simplified directly from the value of $k_2 \cong 10^5$ sec^{-1} cited in Section V. This value indicates that a rapid steady-state between A + E and AE is achieved prior to the time course relevant to epcs.

The rate equations following from these reduced and simplified chemical equations are given in Eqs. (A3) and (A4),

$$\frac{d[\mathrm{AR}']}{dt} \cong k_1^{R^*}[\mathrm{R}^0][\mathrm{A}] - k_{-1}^{R^*}[\mathrm{AR}'] \tag{A3}$$

$$\begin{aligned}\frac{d([\mathrm{A}] + [\mathrm{AE}])}{dt} &\cong \left(1 + \frac{[\mathrm{E}^0]}{K_m}\right)\frac{d[\mathrm{A}]}{dt} \\ &\cong -(k_1^{R^*}[\mathrm{R}^0] + k^{E^*}[\mathrm{E}^0])[\mathrm{A}] + k_{-1}^{R^*}[\mathrm{AR}']\end{aligned} \tag{A4}$$

where $k^{E^*} \equiv k_2/K_m$ and $K_m \equiv (k_{-1}^{E} + k_2)/k_1^{E}$ (see Section V). Equations (A3 and A4) contain only two time-dependent variables [AR′] and [A] and can be solved simultaneously by matrix methods (73) to yield the two time constants τ_{I} and τ_{II} which characterize the system. The reciprocal time constants, or reciprocal relaxation times, are given by Eq. (A5)

$$\tau^{-1} = \tfrac{1}{2}b[1 \pm \sqrt{1 - (4c/b^2)}] \tag{A5}$$

where τ_{I}^{-1} corresponds to the positive sign and τ_{II}^{-1}, to the negative sign. The constant terms b and c in Eq. (A5) are expressions involving

the individual rate constants in Eqs. (A3) and (A4) and are defined below.

Although no further simplification is necessary for a precise mathematical description of the time dependence of [AR'] and [A], two further approximations are suggested by the magnitudes of the individual rate constants which simplify the expressions. These approximations require an estimate of the reaction space volume; this estimate is 450 μm^3 for the rat diaphragm end plates (33). Thus for 2×10^7 active sites for both receptor and esterase, the total active site concentration of each protein is 0.75×10^{-4} M within the homogeneous reaction space assumption. The first simplifying assumption is that the quantity $[E^0]/K_m < 1$ and hence is negligible in Eq. (A4). This is equivalent to assuming a negligibly low steady-state [AE]. This assumption is justified by values of $K_{app} \cong 10^{-4}$ M, $k_2 \cong 10^5$ sec^{-1} and $k_3 \cong 2 \times 10^4$ sec^{-1} in Section V, from which one can estimate K_m to be about 6×10^{-4} M and $[E^0]/K_m$ to be about 0.12. With this assumption b and c are given by Eqs. (A6) and (A7).

$$b \cong k_1^R [R^0] + k^E [E^0] + k_{-1}^R \tag{A6}$$

$$c \cong k^E [E^0] k_{-1}^R \tag{A7}$$

sec^{-1} in Sections V–VII, the values of all terms in Eqs. (A6) and (A7) except $k_{-1}^{R^*}$ are determined. An estimate of $k_{-1}^{R^*} = 0.5 \times 10^3$ sec^{-1} from electrophysiological data will be assumed (37,38,66). The second simplifying assumption is that the quantity $4c/b^2 < 1$ such that τ^{-1} in Eq. (A5) can be approximated by the first two terms of a power series as in Eq. (A8).

$$\tau^{-1} \cong \tfrac{1}{2} b[1 \pm (1 - 2c/b^2)] \tag{A8}$$

This assumption is justified by noting the values of $b = 2 \times 10^4$ sec^{-1} and $c = 8 \times 10^6$ sec^{-2}. The time constants τ_I and τ_{II} are now given by Eqs. (A9) and (A10).

$$\tau_I^{-1} \cong b - (c/b) \cong b \tag{A9}$$

$$\tau_{II}^{-1} \cong c/b \tag{A10}$$

Completing the matrix method solution with the boundary condition that at time zero [A] = [A^0], one obtains Eq. (A11) for [AR'].

$$\frac{[AR']}{[A^0]} = \frac{k_1^{R^*}[R^0]}{\tau_I^{-1} - \tau_{II}^{-1}}(e^{-t/\tau_I} - e^{-t/\tau_{II}}) \qquad (A11)$$

The smaller rate constant τ_{II}^{-1} determines the decay phase and according to Eq. (A10) and Eq. (A7) ff. is approximately $k_{-1}^{R^*}$. The maximum value of [AR'] is obtained by differentiating Eq. (A11) and determining the time t_p to peak amplitude [Eq. (A12)].

$$t_p = \frac{\ln(\tau_{II}/\tau_I)}{\tau_I^{-1} - \tau_{II}^{-1}} \qquad (A12)$$

The calculated value of t_p is about 220 μsec. Substitution of t_p into Eq. (A11) gives $[AR']_{max}/[A^0] = 0.082$.

The reduced receptor reaction in Eq. (A1) can be expanded to include a dimeric A_2R' as the only state which corresponds to an open channel (see Fig. 7) as shown in Eq. (A13).

$$2\,A + R \underset{k_{-1}^{R^*}}{\overset{2k_1^{R^*}}{\rightleftharpoons}} AR' + A \underset{2k_{-1}^{R^*}}{\overset{k_1^{R^*}}{\rightleftharpoons}} A_2R' \qquad (A13)$$

If, as indicated by the relative rate constants in Eq. (A13), both acetylcholine binding sites are equivalent and independent, then Eq. (A11) still holds, with the exception that AR' in Eq. (A11) must be replaced by the total receptor-bound acetylcholine, defined as $[A_b] \equiv [AR'] + 2[A_2R']$. Since $[R^0] \gg [AR']$, to a good approximation $[AR'] \gg [A_2R']$. Then $[A_b] \cong [AR']$ and the rate equation for $[A_2R']$ is given in Eq. (A14)

$$\frac{d[A_2R']}{dt} \cong k_1^{R^*}[A][A_b] - 2k_{-1}^{R^*}[A_2R'] \qquad (A14)$$

and integration gives Eq. (A15).

$$\frac{[A_2R']}{[A^0]} = \frac{(k_1^{R^*})^2[A^0][R^0]}{(\tau_I^{-1} - \tau_{II}^{-1})^2}[\tfrac{1}{2}e^{-2t/\tau_I} + \tfrac{1}{2}e^{-2t/\tau_{II}} - e^{-t(\tau_I^{-1}+\tau_{II}^{-1})}] \qquad (A15)$$

It is noteworthy that Eqs. (A11) and (A15) still hold when $[E^0]$ is greatly reduced by an esterase inhibitor. The estimated $[A^0] \cong 1.5 \times 10^{-5}\,M$ is sufficiently below the esterase $K_{app} \cong 10^{-4}\,M$ that the initial approximation $[E] \cong [E^0]$ is still valid when $[E^0]$ is small. If $[E^0]$ is reduced to 1% of its initial value, $b = 2 \times 10^3$ sec^{-1} and $c = 8 \times 10^4$ sec^{-2}. The calculated t_p is 1970 μsec and $[AR']_{max}/[A^0] = 0.66$.

The calculated epc decay rate constant corresponds to τ_{II}^{-1} in Eq. (A11) and to $2\,\tau_{II}^{-1}$ in Eq. (A15). When 99% of the esterase is inhibited,

τ_{II}^{-1} becomes 35 sec^{-1}, somewhat smaller than the rate of diffusion from the synaptic cleft (see Section II); in this case the homogeneous reaction space assumption is not applicable. However, when 90% of the esterase is inhibited, τ_{II}^{-1} becomes 0.21×10^3 sec^{-1}, about half its original value. This calculation appears consistent with electrophysiological observations (37) and suggests that the homogeneous reaction space assumption can be applied to epc decay rate constants at moderate levels of esterase inhibition.

ACKNOWLEDGMENTS

The authors are indebted to Professor David Nachmansohn for stimulating our interest in this field. We also thank Ute Wolfänger for technical help.

This work was supported in part by the Stiftung Volkswagenwerk (Grant 112072) and by the Deutsche Forschungsgemeinschaft (Grant NE 227/1); also by the National Science Foundation (Grants PCM74-08394 and PCM73-00744) and the National Institutes of Health (Grant NS-11766).

REFERENCES

1. Nachmansohn, D. (1955) *Harvey Lect.* **49**, 57–99.
2. Nachmansohn, D. (1959) "Chemical and Molecular Basis of Nerve Activity." Academic Press, New York (revised, 1975).
3. Nachmansohn, D. (1971) *Handb. Sens. Physiol.* **I**, 18–102.
4. Nachmansohn, D. (1968) *Proc. Natl. Acad. Sci. U.S.A.* **61**, 1034–1041.
5. Nachmansohn, D. (1969) *J. Gen. Physiol.* **54**, 197S–224S.
6. Colquhoun, D. (1975) *Annu. Rev. Pharmacol.* **15**, 307–320.
7. del Castillo, J., and Katz, B. (1957) *Proc. R. Soc. London, Ser. B* **146**, 369–381.
8. Rawlings, P. K., and Neumann, E. (1976) *Proc. Natl. Acad. Sci. U.S.A.* **73**, 4492–4496.
9. Neumann, E., Nachmansohn, D., and Katchalsky, A. (1973) *Proc. Natl. Acad. Sci. U.S.A.* **70**, 727–731.
10. Neumann, E., and Bernhardt, J. (1977) *Annu. Rev. Biochem.* **46**, 117–141.
11. Dudai, Y., and Silman, I. (1974) *J. Neurochem.* **23**, 1177–1187.
12. Changeux, J.-P. (1975) *Handb. Psychopharmacol.* **6**, 235–301.
13. Rosenberry, T. L. (1975) *Adv. Enzymol.* **43**, 103–218.
14. Hall, Z. W. (1973) *J. Neurobiol.* **4**, 343–361.
15. McIntosh, C. S. H., and Plummer, D. T. (1973) *Biochem. J.* **133**, 655–665.
16. Lwebuga-Makasa, J. S., Lappi, S., and Taylor, P. (1976) *Biochemistry* **15**, 1425–1434.
17. Rosenberry, T. L., and Richardson, J. (1977) *Biochemistry* **16**, 3550–3558.
18. Koelle, G. B., ed. (1963) "Cholinesterases and Anticholinesterase Agents." Springer-Verlag, Berlin and New York.
19. Bloom, F. E., and Barrnett, R. J. (1966) *J. Cell Biol.* **29**, 475–495.
20. Brzin, M. (1966) *Proc. Natl. Acad. Sci. U.S.A.* **56**, 1560–1563.

21. Fertuck, H. C., and Salpeter, M. M. (1976) *J. Cell Biol.* **69,** 144–158.
22. Salpeter, M. M., Plattner, H., and Rogers, A. W. (1972) *J. Histochem. Cytochem.* **20,** 1059–1068.
23. Rogers, A. W., Darzynkiewicz, Z., Salpeter, M. M., Ostrowski, K., and Barnard, E. A. (1969) *J. Cell Biol.* **41,** 665–685.
24. Ringel, S. P., Bender, A. N., Festoff, B. W., Engel, W. K., Vogel, Z., and Daniels, M. P. (1975) *Nature (London)* **225,** 730–731.
25. Lentz, T. L., Mazurkiewicz, J., and Rosenthal, J. (1977) *Brain Res.* **132,** 423–442.
26. Changeux, J.-P., Kasai, M., and Lee, C. Y. (1970) *Proc. Natl. Acad. Sci. U.S.A.* **67,** 1241–1247.
27. Karlin, A., Prives, J., Deal, W., and Winnik, M. (1971) *J. Mol. Biol.* **61,** 175–188.
28. Miledi, R., and Potter, L. T. (1971) *Nature (London)* **233,** 599–603.
29. Porter, C. W., Chiu, T. H., Wiechowski, J., and Barnard, E. A. (1973) *Nature (London), New Biol.* **241,** 3–7.
30. Berg, D. K., Kelly, R. B., Sargent, P. B., Williamson, P., and Hall, Z. W. (1972) *Proc. Natl. Acad. Sci. U.S.A.* **69,** 147–151.
31. Fambrough, D. M., and Hartzell, H. C. (1972) *Science* **176,** 189–191.
32. Barnard, E. A., and Rogers, A. W. (1971) *In* "Cholinergic Ligand Interactions" (D. J. Triggle, J. F. Morgan, and E. A. Barnard, eds.), p. 175. Academic Press, New York.
33. Salpeter, M. M., and Eldefrawi, M. E. (1973) *J. Histochem. Cytochem.* **21,** 769–778.
34. Bourgeois, J.-P., Kyter, A., Menez, A., Fromageot, P., Boquet, P., and Changeux, J.-P. (1972) *FEBS Lett.* **25,** 127–133.
35. Fatt, P., and Katz, B. (1951) *J. Physiol. (London)* **115,** 320–370.
36. Nastuk, W. L., and Alexander, J. T. (1954) *J. Pharmacol. Exp. Ther.* **111,** 302–328.
37. Magleby, K. L., and Stevens, C. F. (1972) *J. Physiol. (London)* **223,** 173–197.
38. Gage, P. W., and McBurney, R. N. (1975) *J. Physiol. (London)* **244,** 385–407.
39. Anderson, C. R., and Stevens, C. F. (1973) *J. Physiol. (London)* **235,** 655–691.
40. Kordas, S. M. (1972) *J. Physiol. (London)* **224,** 317–332.
41. Katz, B., and Miledi, R. (1973) *J. Physiol. (London)* **231,** 549–557.
42. Magleby, K. L., and Terrar, D. A. (1975) *J. Physiol. (London)* **244,** 467–495.
43. Katz, B. (1969) "The Release of Neural Transmitter Substances." Liverpool Univ. Press, Liverpool.
44. Eigen, M., and DeMaeyer, L. (1963) *Tech. Org. Chem.* **8,** Part 2, 895–1054.
45. Eigen, M., and DeMaeyer, L. (1973) *Tech. Chem. (N.Y.)* **6,** Part 2, 63–146.
46. Winkler-Oswatitsch, R. (1969) Thesis, Göttingen and Vienna.
47. Rosenberry, T. L., and Neumann, E. (1977) *Biochemistry* **16,** 3870–3878.
48. Neumann, E., and Chang, H. W. (1976) *Proc. Natl. Acad. Sci. U.S.A.* **73,** 3994–3998.
49. Chang, H. W., and Neumann, E. (1976) *Proc. Natl. Acad. Sci. U.S. A.* **73,** 3364–3368.
50. Neumann, E., and Chang, H. W. (1978) In preparation.
51. Rieger, F., Bon, S., Massoulié, J., and Cartaud, J. (1973) *Eur. J. Biochem.* **34,** 539–547.
52. Dudai, Y., Herzberg, M., and Silman, I. (1973) *Proc. Natl. Acad. Sci. U.S.A.* **70,** 2473–2476.
53. Massoulié, J., and Rieger, F. (1969) *Eur. J. Biochem.* **11,** 441–455.
54. Hall, Z. W., and Kelly, R. (1971) *Nature (London), New Biol.* **232,** 62–63.
55. Betz, W., and Sakmann, B. (1973). *J. Physiol. (London)* **230,** 673–688.
56. Wilson, I. B., and Cabib, E. (1956) *J. Am. Chem. Soc.* **78,** 202–207.
56a. Rothenberg, M. A., and Nachmansohn, D. (1947) *J. Biol. Chem.* **168,** 223–231.
57. Rosenberry, T. L. (1975) *Proc. Natl. Acad. Sci. U.S.A.* **72,** 3834–3838.
58. Augustinsson, K. B. (1963) *In* Cholinesterases and Anticholinesterase Agents" (G. B. Koelle, ed.), p. 89. Springer-Verlag, Berlin and New York.
59. Aldridge, W. N., and Reiner, E. (1969) *Biochem. J.* **115,** 147–162.

60. Krupka, R. M., and Laidler, K. J. (1961) *J. Am. Chem. Soc.* **83,** 1445–1460.
61. Rosenberry, T. L., and Bernhard, S. A. (1972) *Biochemistry* **11,** 4308–4321.
62. Nolte, H. J., Rosenberry, T. L., and Neumann, E. (1978) In preparation.
63. Gibson, R. E., O'Brien, R. D., Edelstein, S. J., and Thompson, W. R. (1976) *Biochemistry* **15,** 2377–2382.
64. Chang, H. W., and Bock, E. (1977) *Biochemistry* **16,** 4513–4520.
65. Eldefrawi, M. E., Eldefrawi, A. T., Penfield, L. A., O'Brien, R. D., and Van Campen, D. (1975) *Life Sci.* **16,** 925–935.
66. Sheridan, R. Z., and Lester, H. A. (1977) *J. Gen. Physiol.* **70,** 187–219.
67. Katz, B., and Thesleff, S. (1957) *J. Physiol. (London)* **138,** 63–80.
68. Mitchell, J. F., and Krnjevic, K. (1961) *J. Physiol. (London)* **155,** 246–262.
69. Potter, L. T. (1970) *J. Physiol. (London)* **206,** 144–166.
70. Katz, B., and Miledi, R. (1965) *Proc. R. Soc. London, Ser. B* **161,** 483–496.
71. Takeuchi, A., and Takeuchi, N. (1959) *J. Neurophysiol.* **22,** 395–411.
72. Neumann, E. (1974) *In* "Biochemistry of Sensory Functions" (L. Jaenicke, ed.), pp. 465–510. Springer-Verlag, Berlin and New York.
73. Perrin, C. L. (1970) "Mathematics for Chemists," pp. 279–282. Wiley (Interscience), New York.